Approach for the long-term spatial and temporal evaluation of ocean color satellite data products in a coastal environment

P. Jeremy Werdell[a*], Bryan A. Franz[a], Sean W. Bailey[a],
Lawrence W. Harding Jr.[b], and Gene C. Feldman[a]

[a]NASA Goddard Space Flight Center, Greenbelt, Maryland 20771
[b]University of Maryland Center for Environmental Science, Cambridge, Maryland 21613

ABSTRACT

Ocean color satellites provide a mechanism for studying the marine biosphere on temporal and spatial scales otherwise unattainable via conventional in situ sampling methods. These satellites measure visible and infrared radiances, which are used to estimate additional geophysical data products, such as the concentration of the phytoplankton pigment chlorophyll a, C_a, via the application of secondary bio-optical algorithms. The operational C_a algorithms for the Sea-viewing Wide Field-of-view Sensor (SeaWiFS) and Moderate Resolution Imaging Spectroradiometer (MODIS), for example, perform well in the global open ocean, but often degrade in more optically complex coastal environments where global parameterizations are less applicable. Organizations such as the Chesapeake Bay Program, which have interest in using SeaWiFS and MODIS data products to facilitate regional monitoring activities, must rely on locally parameterized algorithms to achieve requisite accuracies. To facilitate algorithm selection, the NASA Ocean Biology Processing Group recently developed the infrastructure to spatially and temporally evaluate a long-term regional time-series of satellite observations using in situ measurements as ground-truth. Here, we present this approach using a case study in the Chesapeake Bay, where a series of C_a algorithms and atmospheric correction schemes were evaluated for the full SeaWiFS and MODIS-Aqua time-series. We demonstrate how the selection of the best algorithms and processing approaches is driven by trade-offs in coverage needs and relative accuracy requirements. While our case study highlights C_a in the Chesapeake Bay, our methodology is applicable to any geophysical data product and region of interest.

Keywords: ocean color, bio-optical algorithm, remote sensing, SeaWiFS, MODIS, Chesapeake Bay

1. INTRODUCTION

Coastal and estuarine waters host a diverse array of benthic and pelagic ecosystems, many of which possess significant commercial and ecological value. Both natural and anthropogenic disturbances, such as sea-level rise, erosion, and industrial and agricultural pollution, alter the biogeochemical characteristics of these ecosystems, frequently resulting in changes in water quality and local habitat structures. Our understanding of how coastal environments respond to such perturbations currently relies on the analysis of long-term (e.g., decadal) time-series of in situ measurements, for example, the Water Quality Monitoring Data[1] collected as part of the Chesapeake Bay Program (CBP) since 1984. The CBP, a cooperative effort between the federal government and state and local governments within the Chesapeake Bay watershed, established 49 stations within the mainstem Bay to be revisited monthly to measure 19 hydrographic and chemical water quality parameters. These data currently provide the scientific foundation for the management of many Chesapeake Bay marine resources.

Ocean color satellites provide a means of complementing field programs with remotely sensed data collected on spatial and temporal scales unachievable by conventional in situ methods. These satellites measure the radiance emanating from the top-of-the-atmosphere at discrete visible and infrared wavelengths. Spectral water-leaving radiances, $L_w(\lambda)$, the light backscattered out of the water mass, are obtained by removing the contribution of the atmosphere from the total signal (a process hereafter referred to as atmospheric correction).[2] The $L_w(\lambda)$ are subsequently used to estimate a number of geophysical data parameters, such as the concentration of the

* jeremy.werdell@nasa.gov, Science Systems and Applications, Inc., Lanham, Maryland 20706

Coastal Ocean Remote Sensing, edited by Robert J. Frouin,
Proc. of SPIE Vol. 6680, 66800G, (2007) · 0277-786X/07/$18 · doi: 10.1117/12.732489

phytoplankton pigment chlorophyll a, C_a, and marine absorption and scattering coefficients, via the application of secondary bio-optical algorithms.[3,4]

The standard bio-optical algorithms of the Sea-viewing Wide Field-of-view Sensor (SeaWiFS) and Moderate Resolution Imaging Spectroradiometer aboard the Aqua spacecraft (MODISA) perform well in the open ocean, but often degrade in optically complex coastal environments.[5] These algorithms use empirical correlations derived from global in situ data sets and, therefore, best describe only the average relationship between L_w and the geophysical data parameter. They cannot account for systematic differences in the bio-optical relationship that may temporarily or permanently exist in certain geographic zones. Organizations such as the CBP, which have interest in using SeaWiFS and MODISA data products to facilitate their regional monitoring activities, therefore, often rely on locally parameterized algorithms to achieve their defined accuracy requirements.

In response to such needs, the NASA Ocean Biology Processing Group (OBPG) recently developed the infrastructure to spatially and temporally evaluate long-term regional time-series of satellite observations to quantify local algorithm performance, using in situ measurements as ground-truth. Here, we present this approach using a case study in the Chesapeake Bay, where a series of C_a algorithms and atmospheric correction schemes are evaluated for the full SeaWiFS and MODISA time-series. We begin with a brief review of two typical C_a algorithmic forms, followed by an explanation of satellite and in situ data acquisition and preparation. We then describe a series of satellite-derived C_a evaluation metrics and analyses, accompanied by example results. Ultimately, we demonstrate how the selection of the best algorithms and processing approaches is driven by trade-offs in coverage needs and relative accuracy requirements. While our case study highlights C_a in the Chesapeake Bay, it is important to note that this methodology is widely applicable to any geophysical data product and region of interest.

2. BIO-OPTICAL ALGORITHMS

Typically, bio-optical algorithms adopt one of two forms: empirical expressions that are derived through the statistical correlation of coincident in situ radiometry and a biogeochemical product of interest; or semi-analytical expressions, where a simplified form of the radiative transfer equation is inverted to retrieve the product of interest. A myriad of examples exist for both forms, all of which maintain their own strengths and weaknesses

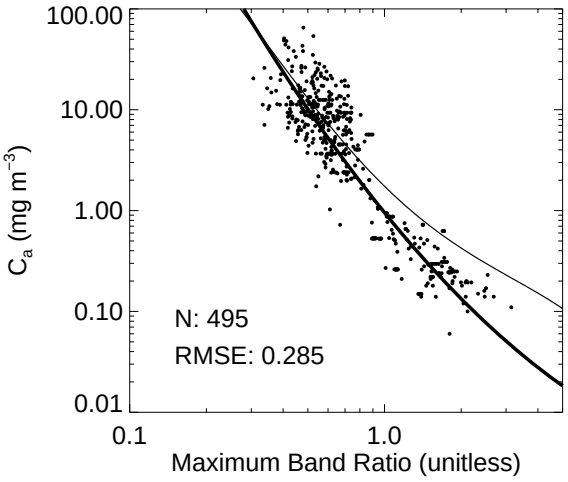

Figure 1. Chesapeake Bay C_a shown as a function of its corresponding R_{rs} maximum band ratio (defined in the manuscript text). The globally parameterized OC3 and regionally tuned OC3-CB are indicated by the thin and thick lines, respectively. With regards to the derivation of OC3-CB, the sample size (N) and root mean square error (RMSE; the root of the residual mean square, in units equal to that of the observation) are also provided.

Table 1. Coefficients for OC3.

	c_0	c_1	c_2	c_3	c_4
OC3 (SeaWiFS)	0.2409	-2.4768	1.5296	0.1061	-1.1077
OC3 (MODISA)	0.2254	-2.6354	1.8071	0.0063	-1.2931
OC3-CB	-0.0208	-3.1263	0.9575		

for coastal remote sensing. Here, we present results for both types of algorithms, but for brevity, only include one globally tuned and one regionally parameterized example of each. A brief description of the specific C_a algorithms under consideration follows.

The operational MODISA empirical C_a algorithm, OC3, is the polynomial best fit when relating log-transformed C_a to a log-transformed ratio of remote sensing reflectances, R_{rs} (the ratio of L_w to downwelling surface irradiance):

$$log_{10}(C_a) = c_0 + \sum_{i=1}^{N} c_i \, log_{10}\left(\frac{R_{rs}(\lambda_b)}{R_{rs}(\lambda_g)}\right) \tag{1}$$

In Eq. (1), λ_b is the greater of $R_{rs}(443)$ and $R_{rs}(488)$ and λ_g is $R_{rs}(551)$. Note that 490 and 555-nm are used in lieu of 488 and 551-nm, respectively, in the SeaWiFS version of OC3. The coefficients c_i are provided in Table 1, and were statistically derived using a global in situ set of coincident C_a and R_{rs}.[3] For comparison, we derived a Chesapeake Bay-specific expression, OC3-CB, using a similar data set[6] with stations limited to those inside the Bay or just outside the mouth of the Bay (Figure 1).

In contrast, the semi-analytical approach relates spectral inherent optical properties to radiances via a polynomial expansion of the spectral ratio $b_b/(a+b_b)$, where $a(\lambda)$ and $b_b(\lambda)$ are the marine absorption and backscattering coefficients, respectively.[7] These spectral coefficients are commonly partitioned into components via $(a = a_w + a_\phi + a_{dg})$ and $(b_b = b_{bw} + b_{bp})$, where the subscripts w, ϕ, dg, and p indicate water (known), phytoplankton, non-phytoplankton particles + dissolved organics, and total particles, respectively. Note that the a_{dg} combination cannot currently be decomposed into its two components via remote sensing methods. In the Garver-Siegel-Maritorena[4] model (GSM), for example, the components are further expanded into:

$$a_\phi(\lambda) = C_a \, a^*_\phi(\lambda), \tag{2}$$

$$a_{dg}(\lambda) = a_{dg}(443) \, exp\left[-S(\lambda - 443)\right], \tag{3}$$

$$b_{bp}(\lambda) = b_{bp}(443) \, (\lambda/443)^{-\eta}, \tag{4}$$

where a^*_ϕ is the C_a-specific absorption coefficient, S is the spectral decay constant for dg absorption, and η is the power-law exponent for the particulate backscattering coefficient. In GSM, these three terms are assigned constant values. Using the spectral satellite radiances as input, the Levenberg-Marquardt nonlinear least-squares procedure is employed to solve for the remaining unknown terms, namely C_a, $a_{dg}(443)$, and $b_{bp}(443)$. As for OC3, the operational constants in Eqs. (2) − (4) were derived using a global in situ data set. For comparison, we also consider the regionally and seasonally parameterized version of this algorithm, GSM-CB, that is presented in Magnuson and co-authors.[8]

Table 2. Thresholds for spatial and temporal stratification.

Spatial (Latitude)		Temporal (Day Numbers)	
Upper Bay	$> 38.6°$N	Spring	$80 - 172$
Middle Bay	$37.6° - 38.6°$N	Summer	$173 - 266$
Lower Bay	$< 37.6°$N	Fall	$267 - 355$
		Winter	$1 - 79$, $356 - 365$

3. DATA ACQUISITION AND PREPARATION

3.1 Satellite data

Approximately 3,000 MODISA and 6,200 SeaWiFS extracted Level-1A files containing all or part of the Bay were acquired from the online OBPG Data Processing System (http://oceancolor.gsfc.nasa.gov/cgi/browse.pl). Both data sets provide $\sim$1.1 km^2 spatial resolution at nadir (SeaWiFS data were limited to Merged Local Area Coverage files). We considered the full time-series for both sensors, specifically June 2002 to March 2007 for MODISA and September 1997 to March 2007 for SeaWiFS. The satellite extract files were made slightly larger than the Bay (35.5 to 40.5°N and -77.5 to -72.5°W) to facilitate subsequent offshore analyses.

Level-2 files were generated using MSL12 version 5.6.2 (http://oceancolor.gsfc.nasa.gov/DOCS/MSL12/). We initially applied the operational atmospheric correction scheme,[2] including the corrections for near infrared water-leaving radiances, bi-directional reflectance, and spectral band-pass effects.[9,10] The Gordon and Wang[2] approach uses two near-infrared (NIR) radiances for aerosol type selection. An alternative approach that uses two shortwave infrared (SWIR) radiances[11] was also considered, the rationale for which will be discussed later. The operational pixel-masking scheme for each sensor was adopted, with the exception that pixels with stray light contamination were retained.[10] We generated one Level-2 file for each candidate C_a product, such that the C_a-specific Level-2 flags were associated solely with that algorithm. We also generated Level-2 files with $L_w(\lambda)$, the downwelling diffuse attenuation coefficient at 490-nm, the aerosol optical thickness at 865-nm, and GSM-derived $a(443)$ and $b_b(443)$.

Prior to data analysis, we applied quality control metrics to the satellite files to ensure that only the most reliable data would be considered. We first applied an automated screening mechanism. Scenes were eliminated if: (a) any pixel within the Bay had a satellite zenith angle greater than 54° (the confidence limit for the atmospheric correction); or (b) fewer than 25% of all Bay pixels were cloud free, as determined by the Level-2 cloud and ice flag. We then visually inspected the remaining scenes to determine their suitability for this analysis. In general, we removed scenes with large off-Bay cloud fronts or sporadic, discontinuous Bay coverage (also resulting from irregular, but significant cloud cover). In the end, 1,107 SeaWiFS and 537 MODISA files remained for our analyses, or approximately nine days of data per month for each sensor.

3.2 In situ data

We acquired approximately 15,750 discrete fluorometric C_a samples collected by participants in the CBP.[1] These data were supplemented with approximately 2,300 independent fluorometric C_a samples collected as part of the NASA Sensor Intercomparison and Merger for Biological and Interdisciplinary Oceanic Studies Program[12] (SIMBIOS; Figure 2). With regards to the latter, high performance liquid chromatography (HPLC) samples were also available, but reserved for subsequent analyses to minimize methodological biases between the two data sets. Given the turbidity of the Bay, and resulting shallow optical depths, only near-surface samples were considered (those collected no deeper than 1-meter). Replicate samples were averaged. Additional details regarding the treatment of the in situ data are provided in Werdell and Bailey.[6]

3.3 Data stratification and post-processing

Given its spatial and temporal variability, we regionally and seasonally stratified the Bay following Magnuson and co-authors[8] prior to comparing the satellite and in situ C_a (Figure 2, Table 2). The Chesapeake Bay has a known annual cycle of phytoplankton, including a progression of dominant species. This stratification precluded the combination of, for example, the winter-spring bloom (diatom-rich) with the summer maxima (picoplankton-rich), which would otherwise complicate interpretation of our results.[13] Spatially and temporally variant sources of terrestrially derived dissolved and particulate matter further confound the bio-optical properties of the Bay.[14]

We generated regional histograms and time-series as vehicles for comparing the satellite and in situ C_a data. Only retrievals within $0.001 < C_a \leq 100$ mg m^{-3} were considered, as, in general, this is the effective operational range of the algorithms under considerations.[3] For the in situ data, only 24 of the 18,000 available stations had values greater than 100 mg m^{-3}. On the contrary, 52 and 8 stations had C_a less than 1.0 and 0.3 mg m^{-3}, respectively. The lowest in situ C_a recorded was 0.17 mg m^{-3}. When spatially stratifying the satellite data, we further excluded retrievals when sample sizes for a given region were less than 200 valid (unmasked) marine pixels. The histograms were generated in lognormal space with a bin size of 0.05. For the satellite time-series, we recorded the mean, median, standard deviation, and sample size of all valid marine pixels for each geographic region for each scene. We later used these values to calculate weighted monthly averages (via the sample sizes). For comparison, we calculated the monthly mean, median, and standard deviation of all in situ stations. The use of monthly averages improved visual clarity in these plots and, in general, eliminated anomalous C_a retrievals.

For each C_a data product, coincident Level-2 satellite and in situ values were statistically compared using the OBPG satellite data product validation system.[5] Briefly, we retained their temporal threshold for coincidence of ± 3-hours. Satellite C_a values were determined as the filtered median of all valid pixels within a 5x5 pixels box centered on the in situ target. Satellite pixel exclusion criteria and additional satellite homogeneity tests are graphically described in Figure 1 of Bailey and Werdell.[5]

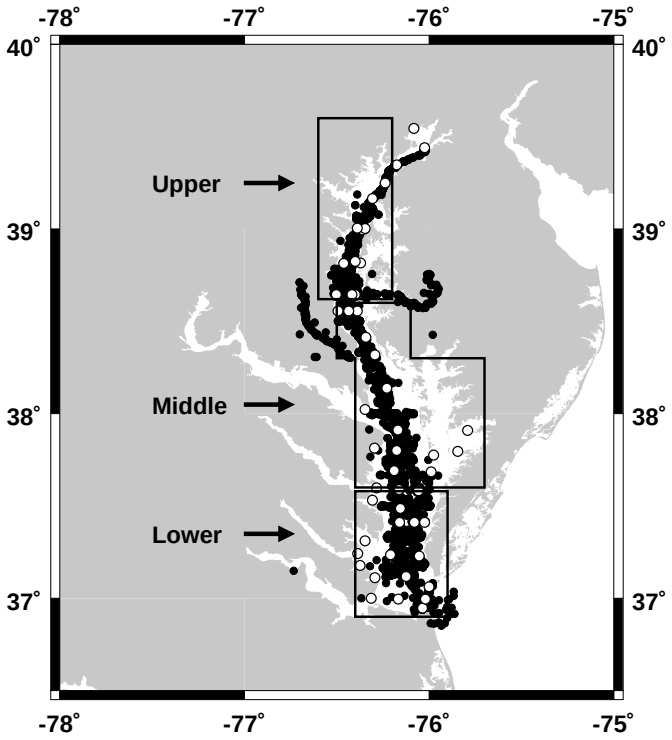

Figure 2. Locations of in situ C_a within the Chesapeake Bay and boxes denoting our adopted regional designations. The CBP[1] and SIMBIOS[12] data sets are indicated by empty and filled circles, respectively.

4. DATA ANALYSIS

Here, we discuss the analyses proposed in Subsection 3.3, describing their relative diagnostic capabilities for algorithm evaluation. For several, we limit the introduction of results to those for either SeaWiFS or MODISA, or for a specific Chesapeake Bay region or season. As our primary purpose is the presentation of the OBPG regional data processing and analysis infrastructure, a detailed interpretation of results is beyond the scope of this document. Rather, we outline the strengths and weaknesses of the analyses as they relate to the coastal remote sensing and marine resource management paradigms.

4.1 Spatial coverage

An examination of the spatial extent of valid satellite retrievals provides an elementary means of determining the utility of a remote sensing algorithm. Naturally, the particular needs of the resource manager dictate the minimum acceptable spatial coverage and its associated frequency of recurrence. Within the mainstem Chesapeake Bay, the empirical algorithms return a greater number of valid Level-2 (daily) pixels than the semi-analytical approaches, as the latter fail in the presence of negative L_w at any wavelength (Figure 3). Note, we continue to consider only retrievals within $0.001 < C_a \leq 100$ mg m^{-3} to be valid, and clouds equally confound both algorithmic forms. Negative L_w commonly occur in the presence of absorbing aerosols, which currently cannot be detected by the atmospheric correction process. This misinterpretation of aerosol type leads to underestimates of blue L_w, where the signals are already low because of high a_{dg} (and a_ϕ to a lesser degree) in that spectral region. With regards to Level-2 spatial coverage, the empirical algorithms perform better, as they return viable C_a when only 488 and 555-nm are available. These sample size differences will be evident throughout the analyses presented in Section 4.

With regards to increasing spatial coverage, two other points merit discussion. First, the regionally parameterized versions of each algorithm return an increased number of C_a within 0.001 to 100 mg m^{-3} (Figure 3). These algorithms were developed using regional in situ data, leading to realistic algorithm boundary conditions, whereas their global counterparts were developed using data atypical of the Bay. Second, the spatial and temporal aggregation[15] of the Level-2 data into Level-3 monthly averages equalizes the relative spatial coverage of the empirical and semi-analytical algorithms. Considering the ten SeaWiFS Level-2 scenes from April 2006, for example, GSM-CB returns valid C_a for an average of 45% of available cloud-free ocean pixels. When Level-3 data are generated at 2 and 4-km spatial resolution using these ten daily files, the percentages rise to 65 and 75%, respectively. Such binning may be useful for regional managers without constraints on temporal and spatial resolution. While we provide results for Level-3 files generated at 2 and 4-km resolution in our latter example, a full discussion of resolution choices in Level-3 binning is beyond the scope of this document.

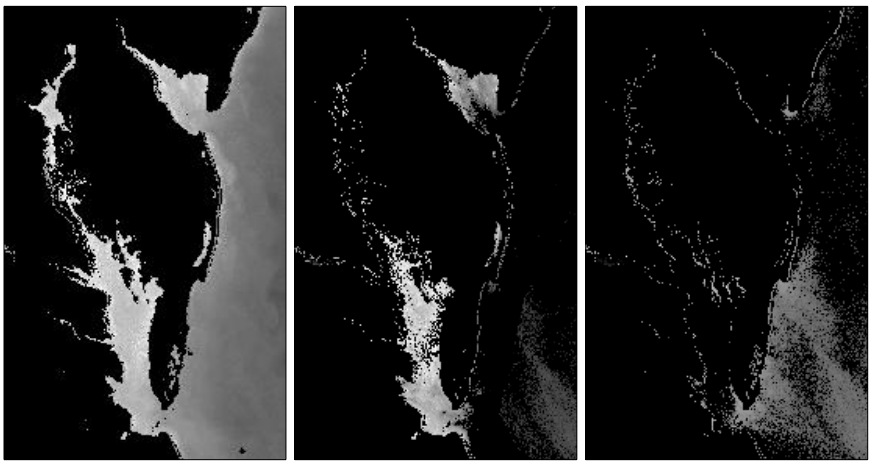

Figure 3. Typical spatial coverage for OC3-CB, GSM-CB, and GSM (from left to right). Black pixels indicate land, clouds, and invalid C_a retrievals. Grey pixels indicate valid retrievals. OC3 is not shown as its coverage mimics that of OC3-CB. SeaWiFS collected these data on 18 April 2006, which was cloud-free over the Bay.

4.2 Level-2 satellite-to-in situ validation

The comparison of coincident satellite and ground truth (e.g., in situ) observations provides a simple, independent means of determining the accuracy and precision of the satellite data products. Within the Bay, the global OC3 and GSM algorithms maintain significant positive and negative biases, respectively, both of which disappear after the application of their regionally-parameterized counterparts (Figure 4). The regional algorithms also show reduced absolute median percent differences relative to the in situ measurements. Note that the positive OC3 bias is consistent with that reported by Harding and co-authors.[16]

While these results meet expectations, our interpretation is truly valid for only the range of environmental conditions under which the "matchups" were acquired (e.g., relative water turbidity and solar and satellite geometries). Unfortunately, our results are hampered by diminutive sample sizes, despite the spread of matchup stations throughout the full mainstem Bay. Recall, we applied the global exclusion criteria and thresholds of the operational OBPG validation system, rather than optimizing these parameters for a turbid estuary. Conceivably, a 5x5 satellite pixel box is inappropriately large, or the ± 3-hours temporal coincidence threshold too restrictive for such an analysis. Bailey and Werdell[5] statistically justified the global optimization, and our ongoing Bay-specific parameterizations have adopted a similarly conscientious approach. Following our above example, while Bay patchiness might dictate, for example, a 3x3 pixel box, the uncertainty about the mean C_a that has been derived from valid pixels within this box will increase in accordance with the decreased sample size.

4.3 Distributions

Comparison of frequency distributions provide a mechanism for revealing relative biases and differences in dynamic ranges amongst multiple coincident data sets. Here, coincidence is defined only through season and region, which differs from the Level-2 validation approach presented in the preceding Subsection. For the scenario presented in Figure 5, histogram analyses of the in situ data show C_a to be lognormally distributed within the various Bay regions and seasons, with well-defined dynamic ranges. Despite their sample sizes being inherently larger, the remotely sensed C_a have similarly shaped distributions, with the exception of GSM-CB. The latter returns an increased number of low (< 1 mg m^{-3}) and high (> 100 mg m^{-3}) C_a, effectively flattening its histogram. The similar histogram widths of OC3, OC3-CB, and GSM suggest the breadth of their dynamic range to be consistent, however, OC3 and GSM show positive and negative biases, which is consistent with results presented in Subsection 4.2. In the Lower and Middle Bays, the regionally tuned OC3-CB and GSM-CB show

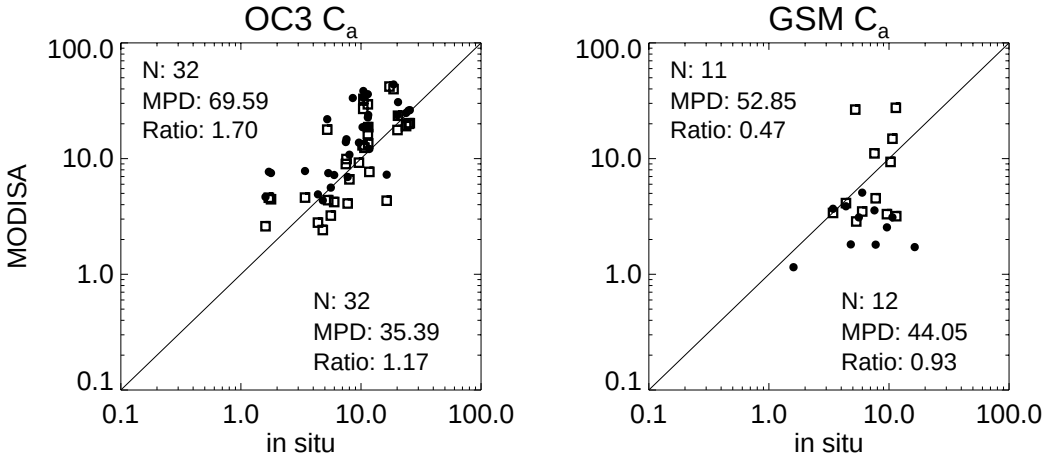

Figure 4. MODISA satellite-to-in situ validation results for the globally (filled circles) and regionally-parameterized (empty squares) versions of OC3 and GSM. Validation statistics for the global and regional algorithms are presented in the upper-left and lower-right corners, respectively, of each panel, where MPD indicates the absolute median percent difference and Ratio the mean satellite-to-in situ ratio.

Table 3. Absolute median percent differences between MODISA and in situ C_a for each season and Bay region. Bold type indicates the minimum difference for scenario. N presents the in situ sample size.

		N	OC3	OC3-CB	GSM	GSM-CB
	Spring	1208	85.7	63.8	85.2	**63.4**
Upper	Summer	1364	44.4	20.8	119.2	**3.3**
Bay	Fall	374	100.6	75.0	**64.6**	82.4
	Winter	717	91.7	68.2	79.9	**62.8**
	Spring	1752	65.4	39.8	104.0	**33.9**
Middle	Summer	1986	51.3	**24.6**	78.5	58.1
Bay	Fall	808	76.3	45.1	87.8	**24.7**
	Winter	1268	91.0	65.4	85.9	**45.4**
	Spring	1993	65.7	**33.0**	95.6	38.1
Lower	Summer	2532	45.2	**10.6**	75.6	58.5
Bay	Fall	1142	45.6	**6.1**	115.9	9.4
	Winter	1537	85.6	54.2	111.5	**45.9**

little bias in comparison to the in situ data, at least with regards to their modes. All of the algorithms under consideration misrepresent the Upper Bay.

We calculated the absolute median percent differences, MPD, between the satellite-derived and in situ C_a for each season and Bay region (Table 3). In this calculation, the geometric means for each scenario are compared, which is prudent given the unimodal symmetry of the lognormally transformed data and the proximity of these values to the distribution modes. Per scenario, the lowest MPD is achieved by a regional algorithm, with the exception of the Upper Bay in the Fall. Further, the Middle and Lower Bays in the Summer are the only other scenarios where a global algorithm outperforms a regional algorithm (OC3 and GSM-CB in both cases). Regionally, GSM-CB has the lowest MPD in the Upper and Middle Bays, despite its broad frequency distributions, while OC3-CB has the lowest MPD in the Lower Bay. For all scenarios, GSM-CB maintains approximately half the sample size of OC3-CB (data not shown).

4.4 Time-series

Time-series comparisons simultaneously display relative biases and seasonal differences amongst multiple coincident data sets. Here, we again define coincidence broadly by Bay region and season. While not desirable, given the needs of a particular data manager, a temporally consistent bias might be qualitatively acceptable if the remote sensing time-series adequately reproduces the local seasonal patterns of the ground truth data. Conceptually, consistent biases are statistically removable via the application of constant offsets. As alluded to in Subsection 3.3, the use of monthly averages in our time-series analyses improved their clarity and, in general, eliminated anomalous C_a retrievals. We explored the use of alternate filtering and statistical smoothing techniques, however, for brevity, they will not be discussed in this paper.

For the Middle Bay, for example, the positive and negative biases of OC3 and GSM, respectively, are again evident in monthly comparisons of satellite-derived and in situ C_a (Figures 6 and 7). Unfortunately, these biases are too large to clearly demonstrate comparable seasonal patterns with the in situ data (suggesting that a constant offset would not align the C_a). In contrast, OC3-CB and GSM-CB show little bias in comparison to the in situ data and similar seasonal patterns with few exceptions (e.g., April 2003). Further, their MPD decrease relative to their global counterparts (note that values shown in Figure 6B and 7B reiterate the values

presented in Table 3). While the sample sizes for GSM-CB significantly exceed those for GSM, they still trail those for the empirical algorithms by approximately 50%.

5. DISCUSSION

The NASA OBPG recently developed the infrastructure to rapidly process and analyze long-term regional time-series of remotely sensed data products. The system is completely independent of satellite sensor, geographic region, and biogeophysical data product, so long as the processing scheme and related algorithms have been incorporated into the OBPG Level-2 processing software MSl12. While in situ data typically provide ground truth, the system also permits satellite-to-satellite, satellite-to-model, and satellite-to-climatology comparisons. In this paper, we present the approach using a C_a-based case study in the Chesapeake Bay. To facilitate regional monitoring activities, the OBPG recently partnered with the CBP to evaluate the quality of SeaWiFS and MODISA C_a retrievals in the Bay using in situ data as ground truth.

A comprehensive discussion of results exceeds the scope of this paper, as our primary intent is the presentation of data analysis approaches, accompanied by a description of the benefits and limitations of each. We consider only four bio-optical algorithms with a single atmospheric correction scheme in Section 4, but stress that a myriad of alternate atmospheric correction options and in-water algorithms are available, all with their own strengths and weaknesses. For example, Wang and Shi[11] propose that the use of SWIR radiances in lieu of NIR radiances improves identification of aerosol type and concentration in turbid waters. The Gordon and Wang[2] atmospheric correction approach requires two $L_w(\lambda) = 0$, a condition met by L_w(SWIR) in turbid water, but not by L_w(NIR). Unfortunately, the on-orbit calibration of the SWIR detectors is less reliable than that for the NIR because of severely low signal-to-noise ratios.

Despite the limited results presented in Section 4, several emerging "lessons learned" merit discussion. First, consider the significant differences in spatial coverage for our candidate empirical and semi-analytical C_a algorithms. Data managers with interest in GSM-CB, either for its reasonable accuracy (see, e.g., Figure 4 and

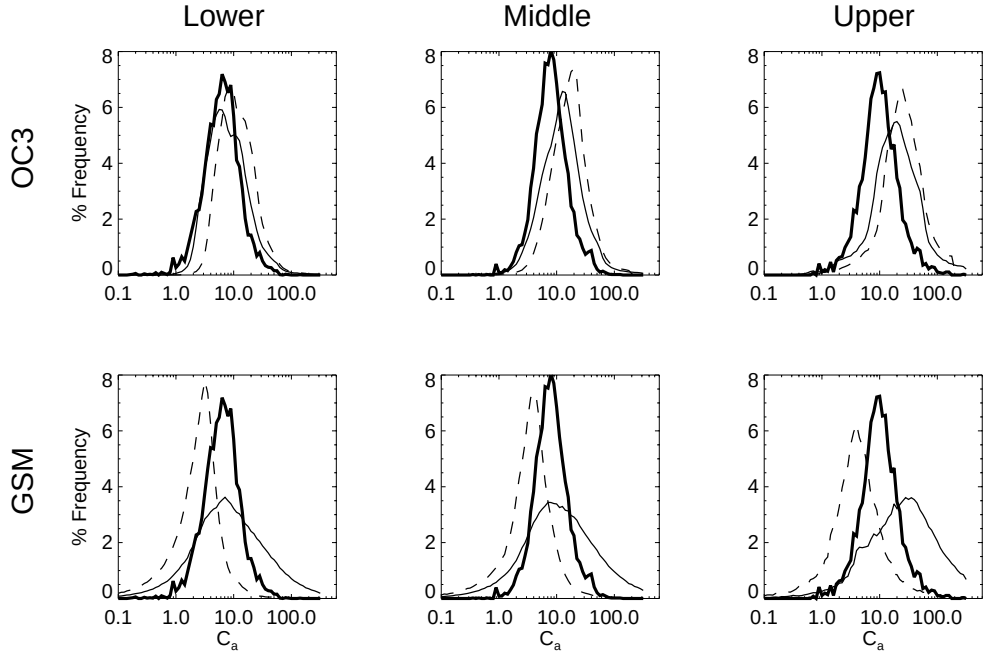

Figure 5. In situ (thick lines) and MODISA-derived C_a distributions in the Lower, Middle, and Upper Chesapeake Bay. The global (thin dashed) and regional (thin solid) versions of OC3 (top row) and GSM (bottom row) are both presented, and data from all four seasons are included.

Table 3) or ability to simultaneously estimate $a_{dg}(\lambda)$ and $b_{bp}(\lambda)$, sacrifice considerable daily spatial coverage in comparison to the empirical algorithms. The generation of Level-3 products increases relative spatial coverage, but sacrifices both temporal resolution (from near-daily to weekly or monthly) and spatial resolution (from pixel widths of approximately 1 to 2 or 4-km). The particular coverage needs and accuracy requirements of the data manager inevitably determine the optimal geophysical algorithms and processing approaches.

Next, results from our specific case study suggest that the standard C_a algorithms employed by SeaWiFS and MODISA benefit from regional parameterization. While it is unreasonable to directly extend this result to

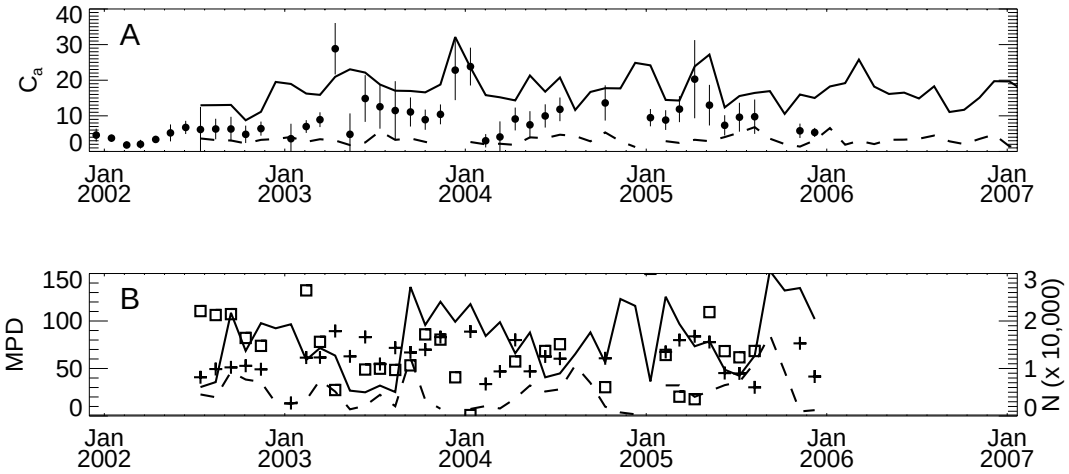

Figure 6. (A) Monthly averages of C_a in the Middle Bay for the in situ data set (filled circles) and the MODISA global OC3 (solid line) and GSM (dashed line). The vertical bars represent one standard deviation about the in situ averages. (B) Absolute median percent differences (MPD) between the satellite and in situ C_a and number of satellite observations (N) for OC3 (squares and solid line, respectively) and GSM (crosses and dashed line, respectively).

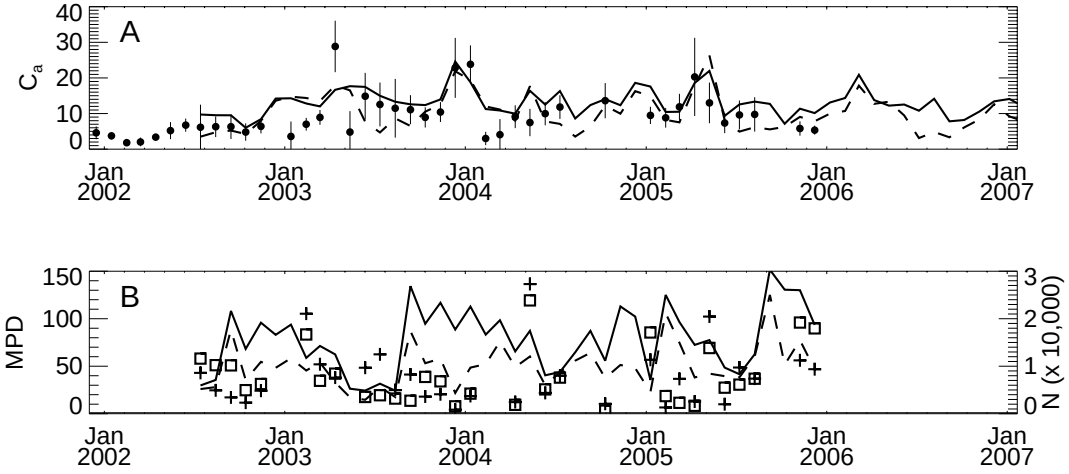

Figure 7. (A) Monthly averages of C_a in the Middle Bay for the in situ data set (filled circles) and the MODISA regional OC3-CB (solid line) and GSM-CB (dashed line). The vertical bars represent one standard deviation about the in situ averages. (B) Absolute median percent differences (MPD) between the satellite and in situ C_a and number of satellite observations (N) for OC3-CB (squares and solid line, respectively) and GSM-CB (crosses and dashed line, respectively).

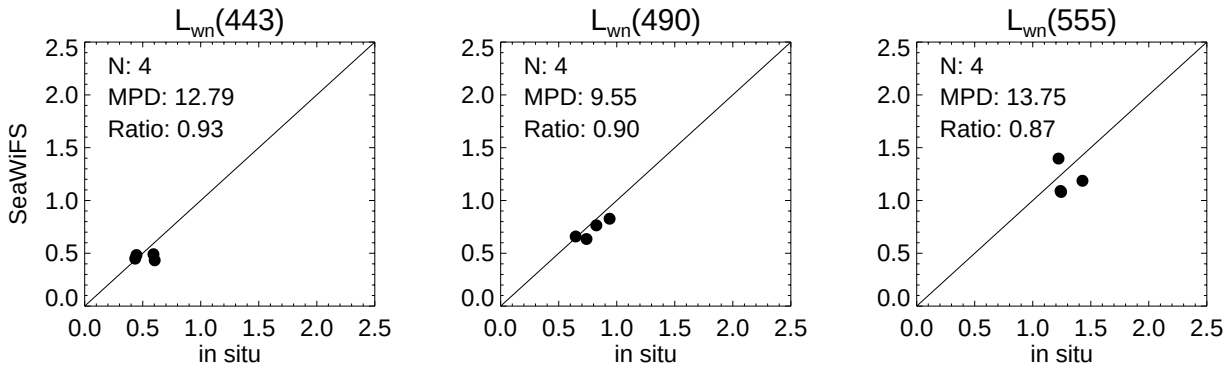

Figure 8. Radiometric validation results for SeaWiFS, with statistics as defined in the Figure 4 caption.

other water masses, we suspect that the quality of those algorithms tuned largely to open ocean measurements will consistently degrade in more optically complex (e.g., coastal) regimes. Regional algorithm tuning, however, is only possible with an abundance of high quality in situ data. In the absence of such data, quantification of algorithm accuracy, precision, and overall uncertainty is still possible via the analyses presented above. In some cases, the statistical evaluation of these results provides sufficient information for regional algorithm adjustment (e.g., the removal of temporally consistent biases or offsets). Alternatively, other remotely sensed products occasionally provide reasonable surrogates for the geophysical product of interest. In our Chesapeake Bay study, we found a reasonable correlation between remotely sensed $a(443)$ and in situ C_a, which is not surprising given the maximum C_a absorption peak at this wavelength (results not shown). While not elaborately discussed in this paper, the need for regional parameterization also extends to the atmospheric correction scheme and to the aerosol types embedded into this scheme (most of which are tuned to maritime rather than urban or coastal conditions).

Finally, the relative quality of the remotely sensed C_a, as well as that of other secondary products, depends largely on the quality of the input $L_w(\lambda)$, which varies significantly from sensor to sensor. Evaluation of satellite radiometric retrievals within the Chesapeake Bay is difficult, however, because of a paucity of coincident, high quality in situ data. Radiometric measurements are not made as part of the CBP Water Quality Monitoring program, so we are limited to those collected as part of SIMBIOS.[12] Despite the limited number of measurements, SeaWiFS appears to perform well in the Lower Bay (Figure 8). Unfortunately, insufficient data were available to retrieve valid MODISA matchups in the Bay. With regards to the analyses presented in Section 4, the relative differences in SeaWiFS and MODISA-derived C_a (not shown) appear because of differences in their respective $L_w(\lambda)$. Recent OBPG SeaWiFS-to-MODISA comparisons, described in Franz and co-authors,[17] indicate that the 3 - 5% differences found in $L_w(\lambda)$ translate to 10 - 20% differences in eutrophic C_a (> 1 mg m^{-3}, typical of that in the Bay). We do not presuppose one sensor to be superior to the other, but rather, simply reveal that differences in the remotely sensed C_a exist and predominantly result from the radiometric characterization of each instrument (rather than their respective C_a algorithms).

Ultimately, the data streams from ocean color satellites have the potential to improve both our scientific understanding of coastal processes and our ability to manage delicate marine resources, if their uncertainties can be rigorously quantified. The ability to rapidly process and evaluate long-term regional time-series of remotely sensed geophysical data products, as described herein, should facilitate significant progress towards this goal.

ACKNOWLEDGMENTS

We thank Michael Mallonee, David Jasinski, and Mark Trice for their advice and assistance with the CBP Water Quality Monitoring data. We also thank Charles McClain, Shawna Karlson, Kevin Sellner, Chris Kinkade, Eric Stengel, Michael Ondrusek, Chris Brown, and the OBPG Data Processing staff for their valuable comments and suggestions at various stages of this project.

REFERENCES

1. Chesapeake Bay Program, *Guide to Using Chesapeake Bay Program Water Quality Monitoring Data*, CBP/TRS 78/92, Chesapeake Bay Program, Annapolis, Maryland, 1993.
2. H. R. Gordon and M. Wang, "Retrieval of water-leaving radiance and aerosol optical thickness over the oceans with SeaWiFS: A preliminary algorithm," *Appl. Opt.* **33**, 443–452, 1994.
3. J. E. O'Reilly and 24 co-authors, *SeaWiFS Postlaunch Calibration and Validation Analyses, Part 3*, NASA Tech. Memo. 206892 Vol. 11, NASA Goddard Space Flight Center, Greenbelt, Maryland, 2000.
4. S. Maritorena, D. A. Siegel, and A. Peterson, "Optimization of a semianalytical ocaen color model for global-scale applications," *Appl. Opt.* **41**, 2705–2714, 2002.
5. S. W. Bailey and P. J. Werdell, "A multi-sensor approach for the on-orbit validation of ocean color satellite data products," *Rem. Sens. Environ.* **102**, 12–23, 2006.
6. P. J. Werdell and S. W. Bailey, "An improved bio-optical data set for ocean color algorithm development and satellite data product validation," *Rem. Sens. Environ.* **23**, 122–140, 2005.
7. H. R. Gordon, O. B. Brown, and M. M. Jacobs, "Computed relationships between the inherent and apparent optical properties of a flat homogeneous ocean," *Appl. Opt.* **14**, 417–427, 1975.
8. A. Magnuson, L. W. Harding Jr., M. E. Mallonee, and J. Adolf, "Bio-optical model for Chesapeake Bay and the Middle Atlantic Bight," *Estuar. Coast. Shelf Sci.* **61**, 403–424, 2004.
9. A. Morel, D. Antoine, and B. Gentilli, "Bidirectional reflectance of oceanic waters: accounting for Ramen emission and varying particle scattering phase fuction," *Appl. Opt.* **41**, 6289–6306, 2002.
10. F. S. Patt and 17 co-authors, *Algorithm Updates for the Fourth SeaWiFS Data Reprocessing*, NASA Tech. Memo. 206892 Vol. 22, NASA Goddard Space Flight Center, Greenbelt, Maryland, 2003.
11. M. Wang and W. Shi, "Estimation of ocean contribution at the MODIS near-infrared wavelengths along the east coast of the U.S.: Two case studies," *Geophys. Res. Let.* , doi:10.1029/2005GL022917, 2005.
12. L. W. Harding Jr. and A. Magnuson, "Bio-optical and remote sensing observations in Chesapeake Bay," in *SIMBIOS Project 2003 Annual Report*, G. S. Fargion and C. R. McClain, eds., 84–97, NASA Tech. Memo. 212251, (NASA Goddard Space Flight Center, Greenbelt, Maryland), 2003.
13. L. W. Harding Jr., M. E. Mallonee, and E. S. Perry, "Toward a predictive understanding of primary productivity in a temperate, partially stratified estuary," *Estuar. Coast. Shelf Sci.* **55**, 437–463, 2002.
14. C. L. Gallegos, T. Jordon, A. Hines, and D. Weller, "Temporal variability of optical properties in a shallow, eutrophic estuary: seasonal and interannual variability," *Estuar. Coast. Shelf Sci.* **64**, 156–170, 2005.
15. IOCCG, *Guide to the Creation and Use of Ocean-Colour Level-3, Binned Data Products*, Reports of the International Ocean-Colour Coordinating Group, No. 4, IOCCG, Dartmouth, Canada, 2004.
16. L. W. Harding Jr., A. Magnuson, and M. E. Mallonee, "SeaWiFS retrievals of chlorophyll in Chesapeake Bay and the mid-Atlantic Bight," *Estuar. Coast. Shelf Sci.* **62**, 75–94, 2005.
17. B. A. Franz and 9 co-authors, "The continuity of ocean color measurements from SeaWiFS to MODIS," *Proc. SPIE* **5882**, doi:10.1117/12.620069, 2005.